

# Next-Generation NATO Reference Mobility Model Complex Terramechanics - Part 2: Requirements and Prototype

Tamer Wasfy  
Advanced Science and Automation Corp.,  
Indianapolis, IN

Paramsothy Jayakumar  
US Army CCDC GVSC, Warren, MI

## Abstract

In part 2 of this paper the Complex Terramechanics (CT) software tools requirements recommended in NATO research task group RTG-248 are presented along with example simulations from a CT prototype software tool which attempts to satisfy the requirements.

## 1. Complex Terramechanics Requirements for NG-NRMM Software Tools

In part 2 of this paper we describe the main requirements (needed capabilities) for NG-NRMM CT and multibody dynamics (MBD) software tools. The main function of those models is to accurately predict the mobility of manned, unmanned, and autonomous ground vehicles of various sizes that are supported by wheels (including rigid wheels, pneumatic tires, and airless tires), tracks (including segmented tracks and continuous belt-type tracks), skis and/or legs while operating on the various types of world-wide terrains, especially soft soil terrains, that are encountered in military applications while carrying any variation allowable of payloads and/or occupants. The following simplifying assumptions can be used in the CT models:

- Soil is isotropic (same response in any direction).
- Soil is homogeneous/uniform (same properties in any location) under the running gear.
- Vehicle loading to the soil is fast so that soil type does not change during the vehicle loading. This includes:
  - Moisture content. Soil mechanical properties dramatically vary with soil water content. Water takes time to drain out or to evaporate from the soil. In general, change in water content in the soil occurs at a longer time scale than the vehicle loading. Therefore we will assume that water content is constant during vehicle loading.
  - Temperature: soil temperature remains constant during loading (except when modeling snow/ice when melting at the interface can significantly affect vehicle mobility).

The combined MBD and CT software tools must have the 14 capabilities described in the following subsections in order to completely satisfy the NG-NRMM CT software requirements. Example simulations from a CT prototype software tool based on the DIS code [1] which attempts to satisfy the requirements are presented along with the requirements to demonstrate that the requirements are achievable in a relatively short term. DIS uses the discrete element method (DEM) to model the soil [2-5], multibody dynamics (MBD) to model the vehicle [6-10], and the finite element method (FEM) to model the tires [9, 11].

### 1.1 Ability to predict the vehicle mobility measures

The combined CT and MBD vehicle models must be able to predict the following vehicle mobility measures which are of interest to the end-users:

1. Speed. Of special interest is the speed-made-good which is the maximum speed of the vehicle in the desired direction while the vehicle is stable and under control, i.e. can be stopped and steered

by the driver. A minimum speed-made-good threshold can be used to predict the GO and NOGO conditions.

2. Rate of fuel/energy consumption and total fuel consumption along the vehicle's path.
3. Engine torque/power.
4. Wheel/track sinkage.
5. Wheel/track slip.
6. Tire deflection.
7. Suspension system deflection.
8. Actual and available drawbar-pull.
9. Transmitted vibration power to the vehicle's occupants/payloads.
10. Vehicle components' dynamic stresses and fatigue life.
11. Braking distance.
12. Stability: rollover or wheel lift along any axis due to a steering maneuver and/or operating on side/long slopes.
13. Stability: loss of speed control, including acceleration and/or braking control.
14. Stability: loss of directional control including under- and over-steering.
15. Vehicle control activity.
16. Factors which limit performance.
17. 3D interaction forces exerted by the soil on any vehicle component (e.g. tires, track, underbody, tines, etc.). The forces include tractive (tangential), resistance (tangential), and bearing (normal) forces. The vehicle component can be spatially moving/rotating in any arbitrary 3D path with respect to the soil within the component's allowable speed range.

This includes ability to predict the above quantities along any direction, including:

- 1) Omni value: worst possible value in any direction.
- 2) Up-hill value.
- 3) Down-hill value.
- 4) Side-hill value.
- 5) Along a specified direction.
- 6) Along the traverse direction.

This also includes the ability to predict instantaneous, maximum, minimum, and average value of the above quantities over each terrain cell. The ability to predict each mobility measure can be validated using a full-scale instrumented vehicle. The maximum error between the actual value of each of the above variables and the value predicted using the complex terramechanics model depends on the variable and the application. But as a guideline the required maximum error is  $\pm 10\%$ . The error percentage ( $E$ ) is calculated using:

$$E = 100(v_{exp} - v_{model})/v_{max} \quad (1)$$

where  $v_{exp}$  is the experimental value of the variable,  $v_{model}$  is the model value, and  $v_{max}$  is the maximum practical absolute value of the variable. Some examples of  $v_{max}$  are:

- For wheel sinkage  $v_{max}$  is the tire radius.
- For engine torque  $v_{max}$  is the maximum engine torque.
- For vehicle speed  $v_{max}$  is the maximum operational vehicle speed.

Note that  $E$  is not normalized using  $v_{exp}$  because if  $v_{exp}$  is relatively small, it may result in artificially large error values.

Typical full-scale vehicle tests which can be used to validate that the aforementioned mobility measures can be accurately predicted using the coupled CT soil and MBD vehicle models include:

1. **Operating at a constant speed on a constant positive, negative, or side slope.** The wheel slip, wheel/engine torque, and rut depth (on soft soil) can be compared to the model's prediction. In addition, the vehicle can be slowly accelerated to the maximum possible speed and that speed can be compared to the model's prediction. This test can be conducted on both hard and soft soil terrains.
2. **Drawbar-pull test** (Figure 1). This test is a surrogate test to assess the ability of a vehicle to climb sloped terrains while carrying a payload or pulling trailer or another vehicle. This test is typically performed on soft soil terrains. The test can be performed as follows:
  - Two vehicles are used: the test vehicle in front and a much heavier one behind it. The two vehicles are connected through their drawbars by a stiff steel cable. The main vehicle stays in 1<sup>st</sup> gear.
  - The two vehicles start moving at a slow constant speed of 1 m/s such that the connecting cable is slightly loose (i.e. force in the cable is nearly zero). The main vehicle goes on the test terrain (such as a soft soil pit) and maintains 1 m/s. Since the two vehicles are moving at the same speed the drawbar-pull force stays at zero.
  - The test vehicle tries to slowly accelerate. Because the much heavier vehicle behind it still maintains 1 m/s speed, the test vehicle stays at 1 m/s but the force in the cable (drawbar-pull force) slowly increases along with the wheel slip.
  - When the test vehicle reaches its maximum engine RPM, the maximum slip in 1<sup>st</sup> gear has been reached. This typically is less than 100% slip (because at 100% slip the test vehicle must be stationary). Thus in order to plot the slip versus drawbar-pull all the way to 100% slip, the heavier vehicle starts to brake until a complete stop. The test vehicle will have nearly the same speed as the heavy vehicle. The test vehicle wheel slip increases until it reaches 100% when its speed is zero. The main result of the test which will be compared between experiment and simulation is the drawbar-pull coefficient (draw-bar pull force divided by the vehicle weight) versus tire/track slip (e.g. Figure 2). In addition, the actual rut depth as a function of slip can also be compared with the simulation.



**Figure 1** Snapshot from a DIS drawbar-pull simulation for a wheeled vehicle on a dry fine grained soil.

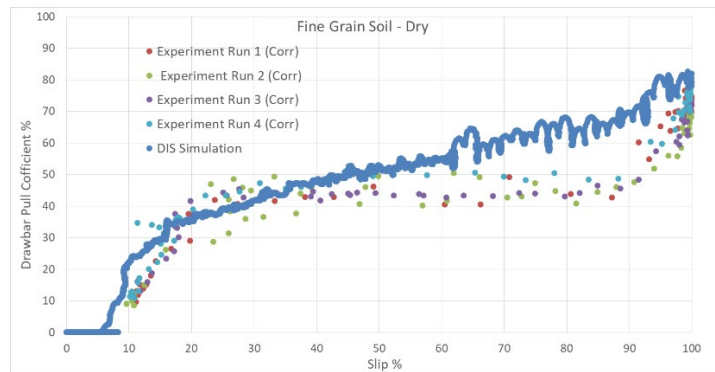


**Figure 2** Test drawbar-pull coefficient versus wheel slip results for a wheeled vehicle and DIS model results (solid blue line) a dry fine grained soil.

3. **Variable (increasing) slope soil climb** (e.g. Figure 3). The vehicle starts on level terrain at a certain target speed. Then, the vehicle tries to maintain this speed as it climbs on an increasing slope terrain. The experiment slope versus wheel slip (Figure 4) and rut depth (for soft soil terrain) for the target vehicle speed can be compared with the simulation.

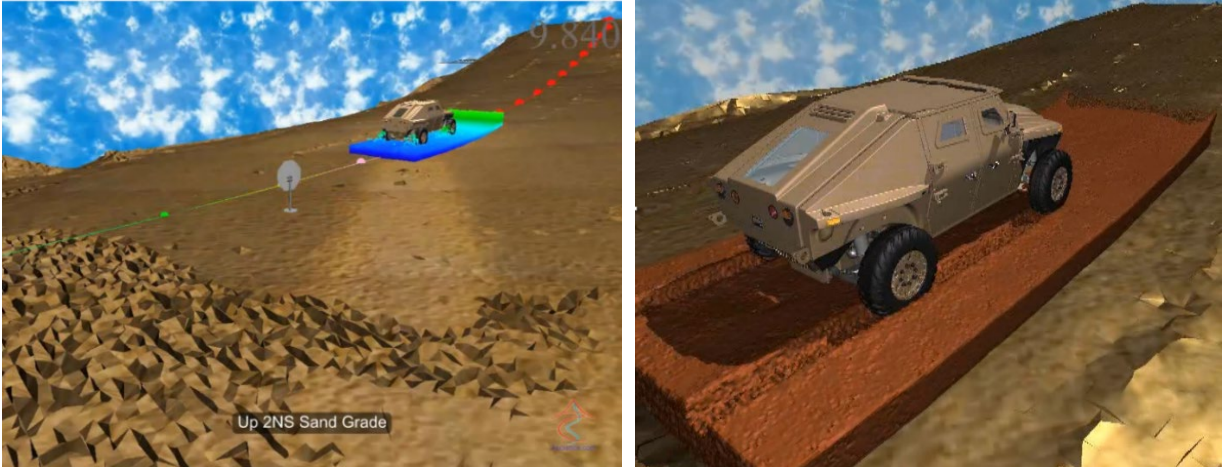


**Figure 3** Snapshots of a DIS simulation of a wheeled vehicle going over a variable sand slope. The slope increases from 0 to 30% in increments of about 5%.

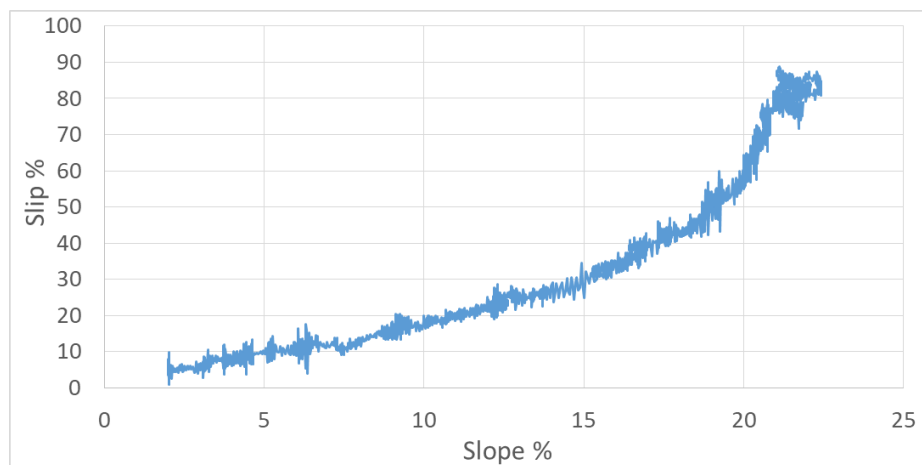


**Figure 4** DIS simulation results of vehicle slip as a function of slope during the sand grade climb (maximum slope reached is about 22%).

### *1.2 Ability to predict terrain deformation/damage caused by the vehicle*

This includes the instantaneous (transient) 3D soil deformation and flow including soil bulldozing in front of the running gear, side rut formation, and separation/reattachment of the soil (Figure 5). It also includes the final resulting terrain deformation, including:

1. Rut depth below the undisturbed soil level.
2. Rut width.
3. Rut shape.
4. Rut side wall height above the undisturbed soil level.
5. Effect of vehicle operation on paved and semi-paved roads and other relatively hard surfaces. This includes:
  - a) Terrain elastic deformation.
  - b) Road/terrain damage. For example, a tank may severely damage urban hard surfaces and make it a rougher terrain for subsequent vehicles.



**Figure 5** DIS simulations of wheeled vehicle on soft cohesive soil showing deep side ruts (left), soil bulldozing in front of the tires (center), and soil separation/reattachment during sinusoidal steering (right).

This includes the ability to predict the above quantities along any direction, including:

- 1) Omni value: worst possible value in any direction.
- 2) Up-hill value.
- 3) Down-hill value.
- 4) Side-hill value.
- 5) Along a specified direction.
- 6) Along the traverse direction.

As a guideline, the maximum error between the actual terrain deformation and that predicted by the CT model is  $\pm 10\%$  and is given by Equation (1).

### *1.3 Ability to accurately predict soil mechanical response for small-scale terramechanics experiments*

In theory, the main advantage of CT models is that they can be calibrated using relatively inexpensive small-scale terramechanics experiments rather than full-scale tire/track and/or full vehicle tests like simple terramechanics or empirical models (such as those used in NRMM). The small-scale terramechanics experiments include:

1. Quasi-static hydrostatic compression using a hydrostatic compression/tri-axial cell or a piston-cylinder uniaxial compression test (Figure 6). The model must be able to reproduce the bulk density versus currently applied hydrostatic pressure (e.g. Figure 7). In addition, the model must be able to reproduce the bulk density versus previously applied hydrostatic pressure curve (i.e. the hydrostatic pressure is applied to compact the soil, then removed and the soil bulk density is measured). The difference between the two curves is the elastic deformation of the soil.

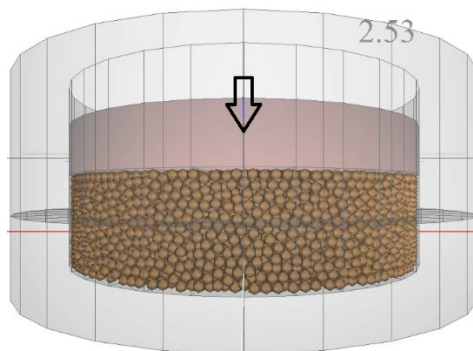


**Figure 6** DIS Simulation of a uniaxial piston-cylinder soil compression test.

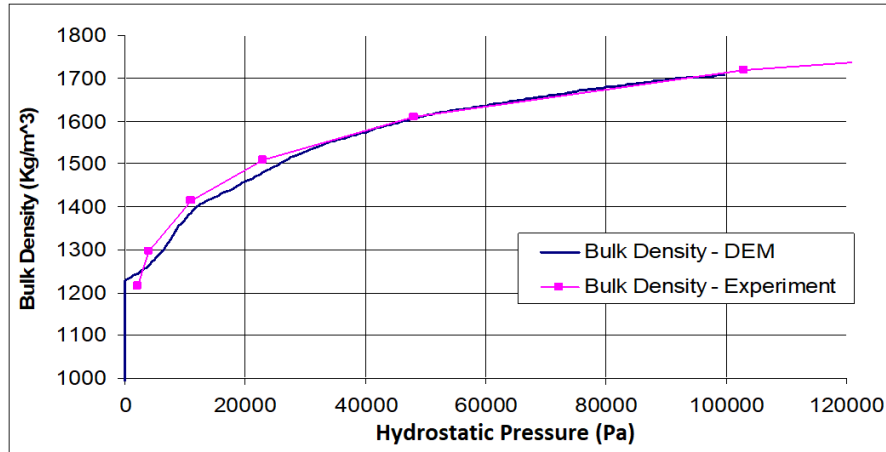


**Figure 7** Comparison between the bulk density versus hydrostatic pressure obtained using a uniaxial piston-cylinder test and a DIS DEM simulation of the test

2. Shear using a shear cell (Figure 8) [12], a triaxial-cell (Figure 9) [13, 14], a rotational bevameter (Figure 10) [15-18], or a translational shear plate (Figure 11) [18]. The model must be able to reproduce the raw experiment results of shear stress versus shear displacement for varying current normal stress and previously applied normal stress when a small quasi-static shear displacement is applied. In addition, the model must be able to reproduce the end experiment results of current normal stress and previously applied normal stress versus maximum shear strength (e.g. Figure 12). The angle that each line in Figure 12 makes with the horizontal axis is the friction angle and the intercept with the vertical axis is the cohesion stress. Note that both the friction angle and cohesion vary with previously applied normal stress, which determines the initial compaction state of the soil. It is also necessary that the model can predict the instantaneous and maximum shear stress at high shear speeds in order to ensure that the model can capture viscous and damping effects in the soil.

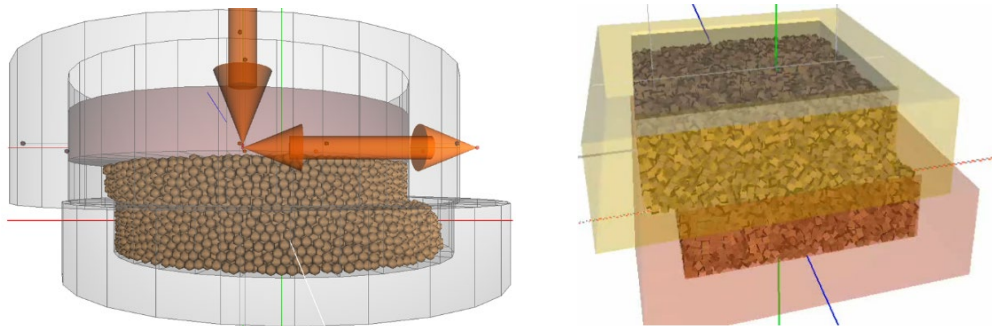


**Figure 8** DIS simulations of cylindrical and cubical shear cells [12, 19, 20].

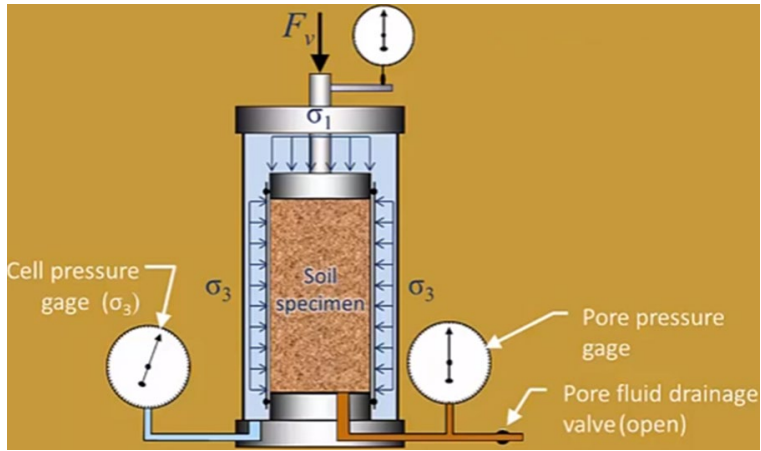


**Figure 9** Tri-axial cell [13, 14].

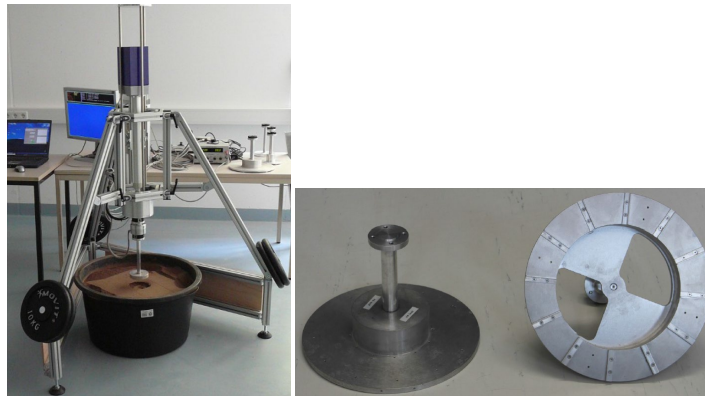


**Figure 10** Rotational Bevameter [15-18].

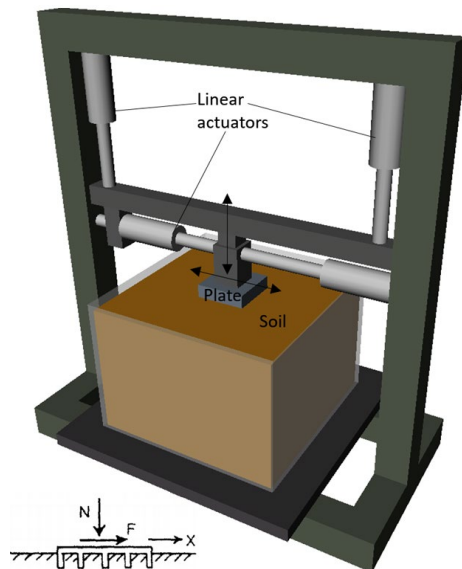


**Figure 11** Translational shear plate [18].

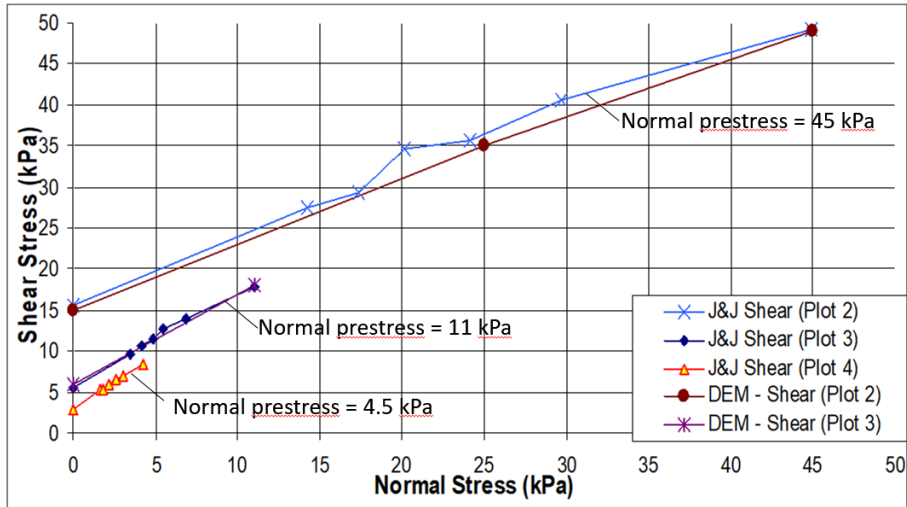


**Figure 12** Comparison of experiment and DIS DEM simulation of shear stress vs. normal stress for different pre-shear normal stress levels (soil compaction levels). The angle between the X-axis and each curve is the soil internal friction angle and the intersection point of the curve with the Y-axis is the soil cohesive shear strength at that pre-shear normal stress value.

3. Penetrometer. The model must be able to reproduce the maximum normal pressure during the penetration into the soil at a prescribed slow speed (quasi-static load) as well the normal force versus penetration distance or time (Figure 13 and Figure 14). The penetrometer can be a standard 30° cone penetrometer [21, 22] (Figure 13) or any other type such as a rectangular plate (Figure 14), a flat cylinder, or a hemisphere [18]. Also, it is necessary that the model can also predict the normal force versus penetration distance or time for different values of penetration speeds up to 10 m/s. This is needed in order to ensure that the soil model can accurately capture damping and viscous effects of the soil.

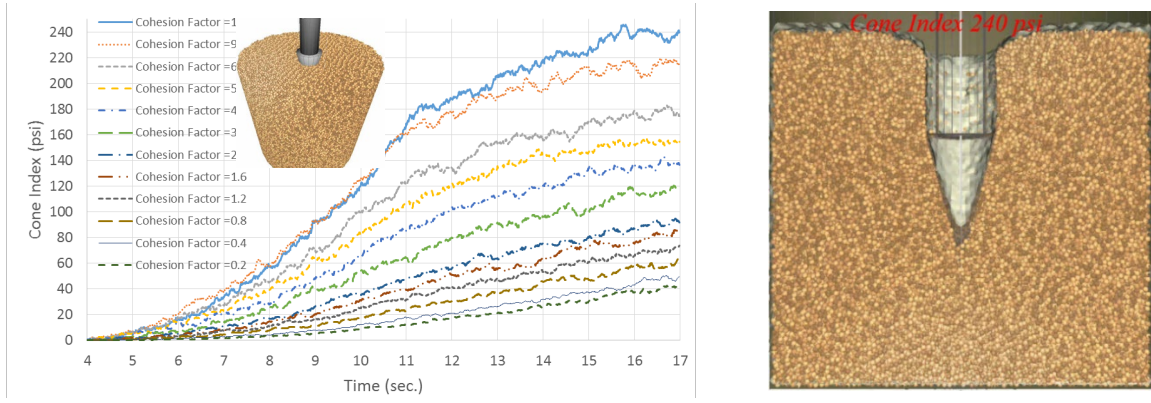


**Figure 13** DIS simulation results of Penetration pressure versus time for 30° angle cone penetrometer. Left figure shows a snapshot of the cone during penetration in a 240 psi (cohesion factor = 12) soil [23].

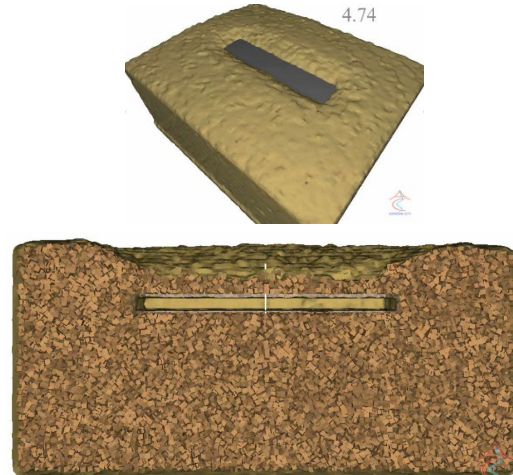
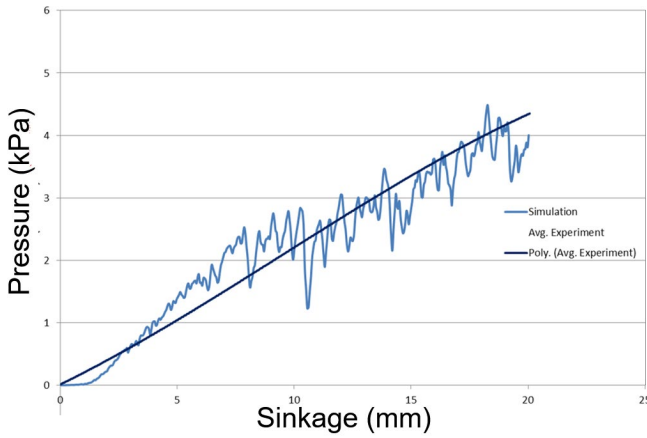


**Figure 14** DIS simulation of penetration pressure versus sinkage for a rectangular penetrometer [19, 20].

- Single rigid wheel (with or without grousers) on soil (Figure 15). The model must be able to reproduce the normal load, slip percentage, and linear speed versus drawbar force and wheel torque (e.g. Figure 16).

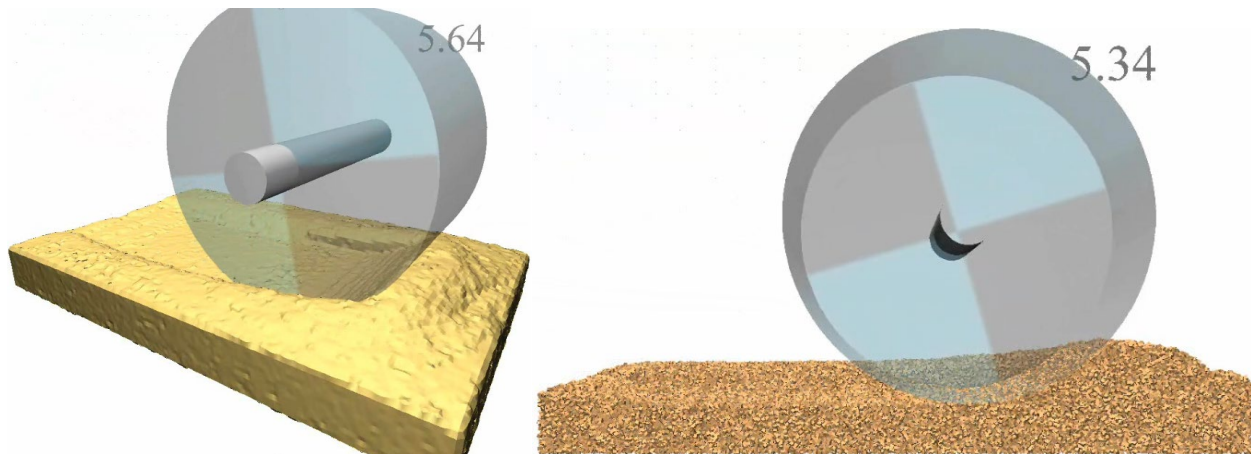


**Figure 15** DIS DEM simulation of a rigid wheel moving on soil [19].

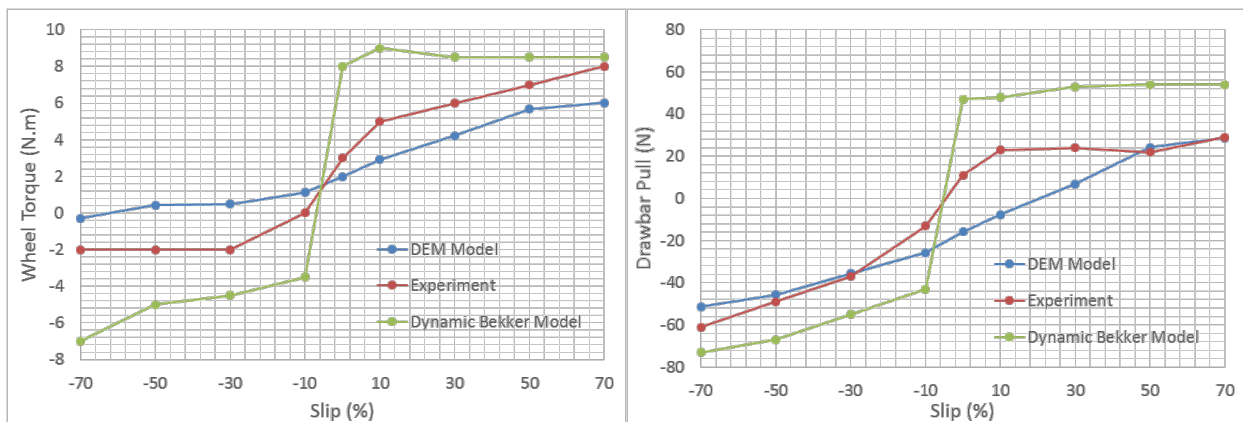


**Figure 16** Comparison between DIS simulation and experiment wheel torque and drawbar pull versus slip for a rigid wheel moving on soil [19, 20].

Those experiments can be modeled using the CT software tool (high-fidelity soil coupled with MBD). Then in order to calibrate the CT models, the CT model parameters are tuned until the simulation and experiments results match.

In addition the CT models must also be able to accurately predict the results of the soil-to-wall surface material terramechanics experiments, including:

- 1) Shear using a wall shear cell or a rotational bevameter (Figure 10) [15-18] or a translational shear plate [18] without grousers (Figure 11). The shearing surface is made out of the vehicle surface material such as rubber or steel. The model must be able to reproduce the end experiment results of current normal stress and previously applied normal stress versus maximum soil - wall shear strength (e.g. Figure 12).
- 2) Soil adhesion to a plate as a function of applied normal stress. The plate is pressed against the soil using a certain normal stress, then the plate is lifted up. The mass of soil which adheres to the plate can be used to estimate the adhesion force between the plate material and the soil (Figure 17).

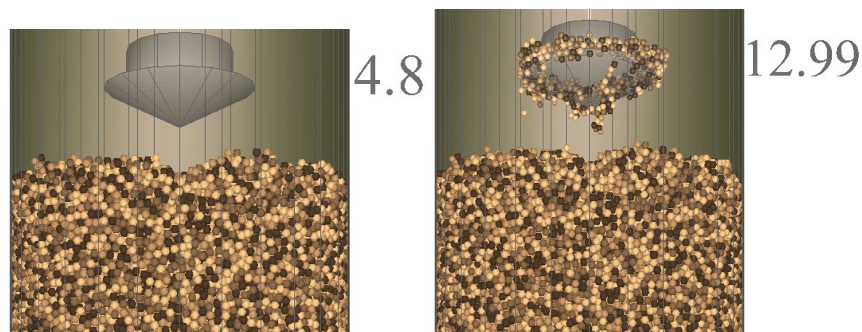


**Figure 17** Snapshots from a DIS DEM simulation of a penetroplate experiment for calibrating the adhesion between the soil and the vehicle running gear (such as tires). The plate is pressed against the soil with a prescribed pressure, then lifted up. The amount of soil stuck to the plate (right snapshot) is proportional to the adhesion force between the plate material and the soil.

As a guideline, the maximum error between the small-scale terramechanics experiments and the complex terramechanics model is  $\pm 10\%$  and is given by Equation (1).

#### *1.4 Ability to reproduce the mechanical response of world-wide soils/terrains*

World-wide soils/terrains include:

1. Natural world-wide soils including all USCS soil types [24]. This also includes the influence of the following physical conditions on the soil mechanical properties:
  - a) Moisture on the soil mechanical properties at and between all Atterberg limits [25].
  - b) Compaction state.
  - c) Temperature including: freezing effects near the water freezing temperature; and effects of high temperatures ( $> 35^\circ$ ) on soil mechanical response especially in dry desert areas.
2. Roads and other hard surfaces including:
  - a) Paved roads with any given 3D geometry, including: asphalt, concrete, brick, and Belgian block. This also includes the ability to represent roads of various decaying conditions.
  - b) Compacted dirt roads including gravel, sand, and clay roads.
  - c) Hard urban surfaces including sidewalks made of brick, rock, or marble.

The mechanical soil response includes the following effects:

1. Traction of the vehicle running gear. This includes friction between the terrain and the running gear and shear strength due to cohesion (Figure 18) and internal friction (Figure 19) and of the soil.

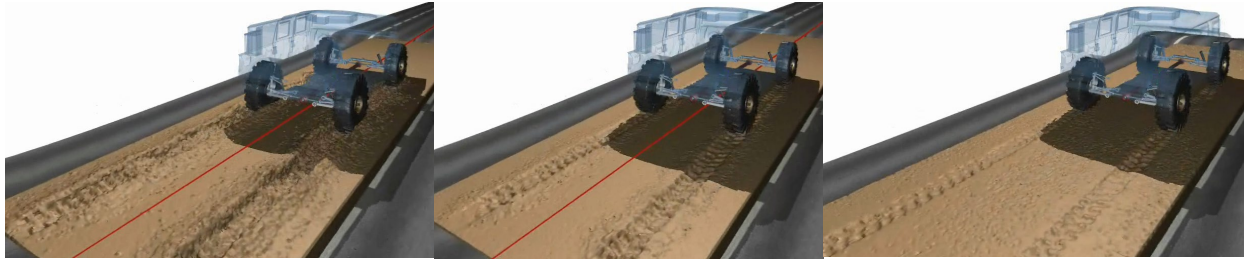


**Figure 18** DIS DEM/MBD simulation of a wheeled vehicle on a level soft soil terrain with low (left), medium (center), and high (right) cohesion soils.

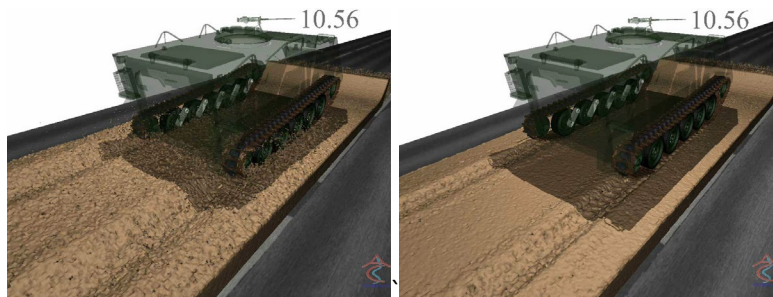


**Figure 19** DIS DEM/MBD simulation of a tracked vehicle for low (left) and high (right) friction soft soils.

2. Change in soil bulk density as a function of soil compaction state (Figure 7). Many soil types including moist soils and soil with organic material content are compressible: soil bulk density decreases with the applied compressive hydrostatic pressure. After removal of the hydrostatic stress, the soil retains most of the deformation (i.e. the residual bulk density is higher than the original uncompressed bulk density) which means the soil has undergone permanent plastic deformation. The maximum currently or previously applied hydrostatic stress determine the soil compaction state.
3. Change in shear strength as a function of soil compaction state (Figure 12). The soil shear strength is a function of the cohesion and internal friction. When soil compaction increases the soil cohesion increases and the internal friction also generally slightly increases due to the fact that when soil is compacted more particles are in contact with each other. Hence soil shear strength increases with soil compaction.
4. Soil dilation is the reduction of bulk density after tilling type loading which includes shearing and/or tension type loading. When soil dilates its' shear strength is reduced compared to compacted soil.
5. Velocity dependent soil forces. It is highly recommended that CT models be able to account for velocity dependent soil forces. Those can also be measured using the small-scale terramechanics tests listed above by applying the normal and/or shear displacement at a controlled speed. Soil normal stress as a function of normal strain rate can be used to calibrate soil damping effects. Soil shear stress as a function of shear strain rate can be used to calibrate soil viscosity effects.
6. Ability to account for adhesion of the soil to the vehicle surfaces (e.g. Figure 20). Typically adhesion between the soil and vehicle surfaces increases with the increase in soil moisture below the soil liquid limit.



**Figure 20** DIS simulation of a vehicle going over a soft soil terrain which includes adhesion between the tires and the soil.

### 1.5 Ability to map physical soil properties into mechanical soil properties then into CT model parameters

Given a soil with a set physical soil properties, namely, USCS soil type, moisture content and temperature, the small terramechanics experiments in Section 1.3 can be used to measure the soil mechanical properties which include: bulk density as a function of hydrostatic stress, cohesive strength as a function of bulk density, friction angle, viscosity coefficient, damping coefficient, dilatency, and elastic constant (Young’s modulus) (Figure 21). In order to enable predicting vehicle mobility over any terrain, a mapping function needs to be developed which maps physical soil properties to mechanical soil properties. This mapping can be based on a database of small-scale terramechanics experiments along with a multivariable interpolation/response surface methodology to find the value of mechanical properties for any combination of soil type, moisture content, and temperature. It is recommended that the minimum soil database consist of: 26 USCS soil types [24], 5 moisture contents (dry, shrinkage limit, plastic limit, and liquid limit), and 5 temperatures (below freezing -10°, at freezing 0°, slightly above freezing 4°, 20° and 40°). This means that the soil database will consist of up to  $26 \times 5 \times 5 = 650$  terramechanics experiments.

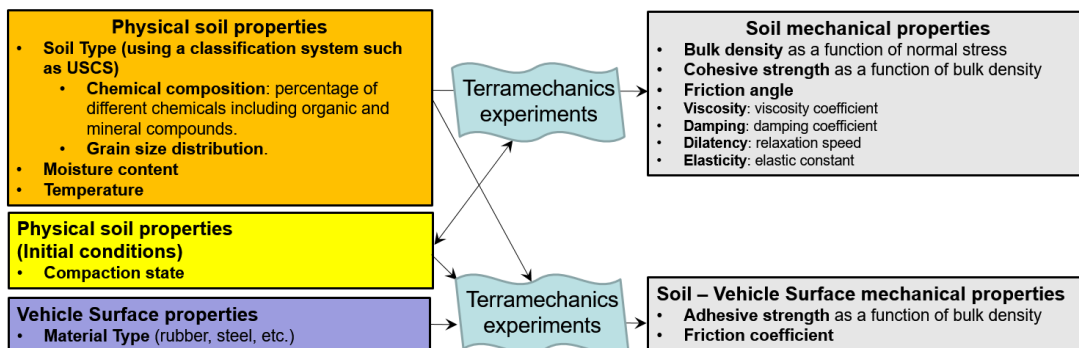


**Figure 21** Mapping of soil physical properties to soil mechanical properties and soil – vehicle surface material mechanical properties required by the complex terramechanics software tool.

After finding the mechanical soil properties for a specific soil, we need to map those properties into the CT model parameters needed to virtually represent the mechanical response of that soil in ground vehicle mobility simulations. This can be done using the following steps (see Figure 22):

1. Assume a set of CT model parameters.
2. Simulate the small-scale terramechanics experiments using the CT models.

3. From the simulated experiments generate the simulated mechanical soil properties.
4. Compare with experiment mechanical soil properties to the simulated mechanical soil properties. If the two match then the set CT model parameters can be used to mechanically represent this soil. Otherwise modify the go to CT model parameters and go to step 1.

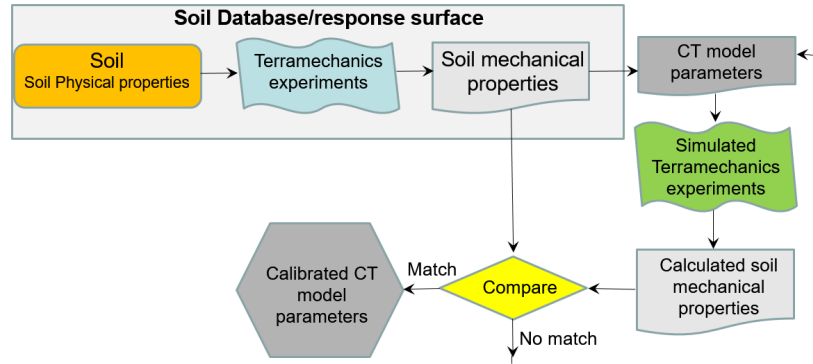


**Figure 22** Mapping of soil mechanical properties to complex terramechanics model parameters.

### 1.6 Ability to represent heterogeneous terrains

Heterogeneous terrains are multi-component terrains which include:

1. Terrains which have discrete patches of different soil type.
2. Terrains with embedded boulders, rocks, stones, and/or gravel (e.g. Figure 20). The effects of soil adhesion and friction at the interface between the soil and discrete terrain component must be accounted for in the model.

The discrete terrain component can be specified by its size, shape, and spacing distributions as well as its mechanical properties.

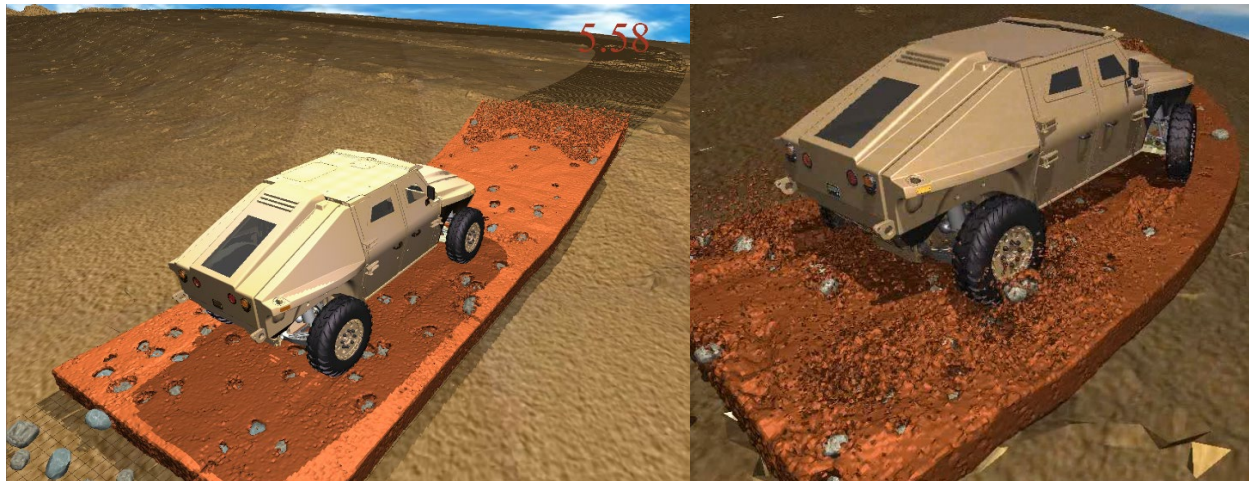


**Figure 23** DIS DEM simulation of a vehicle going over a soft-soil terrain with embedded rocks.

### 1.7 Ability to represent multiple layers of soil

Each layer can have different mechanical properties and each layer can have a different thickness. It is required that the CT software tool support at least 2 soil layers. The layers can include:

- 1) Tilled soil (Figure 24a).

- 2) Organic muskeg layer on compacted soil (Figure 24b).
- 3) Snow and ice covered terrains (Figure 24c). This includes the ability to model transition from snow to ice to water as vehicle passes over snow (melting effects).



**Figure 24** Terrain with a top layer of (a) Tilled soil; (b) Organic muskeg soil; (c) snow.

### 1.8 Ability to represent water covered terrains

This includes fording and swimming vehicles (Figure 25). It includes ability to model the following effects:

1. Representing water resistance to the vehicle motion due to viscosity and inertia.
2. Representing soil entrainment/suspension in the water.
3. Including the effects of air bubble entrainment (can affect vehicle buoyancy) due to rotation/motion of propellers, tires, and vehicle body.
4. Representing the soft soil water bottom which can include: soft organic soil, sand, gravel, etc.
5. Modeling water currents including current speed and direction.
6. Modeling water waves direction and amplitude.
7. Ability to deal with multiple solid bodies moving and deforming arbitrarily in the flow field, and a liquid free surface with surface breakup and reattachment.
8. Ability to model the response/mobility of the vehicle during fording (when the vehicle is propelled by the wheels in contact with bottom soil) and swimming (when the vehicle is fully floating in the water).
9. Modeling propellers and water jets for swimming.
10. Transition of the vehicle from solid terrain to flooded terrain and vice versa.
11. Modeling different types of water bodies including swamps, rivers/streams, lakes, and seas/oceans.

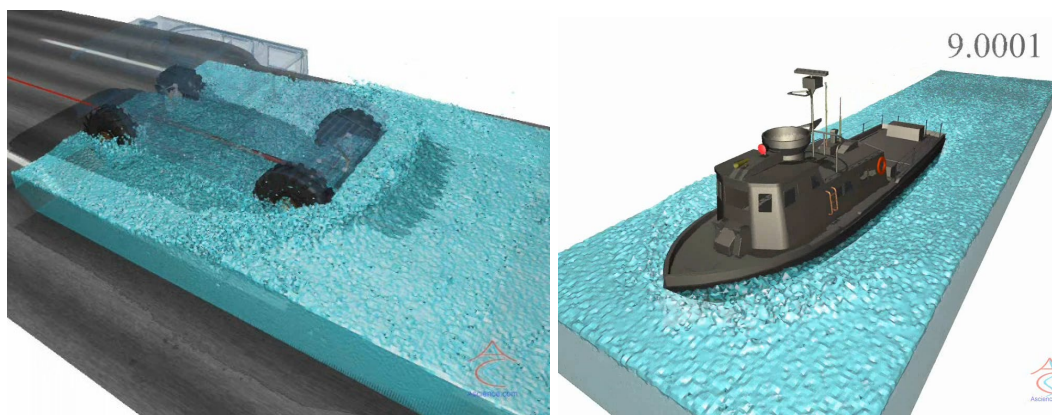


**Figure 25** DIS SPH simulation of water fording [26] (left) and swimming (right).

### 1.9 Ability to model long complex topography terrains

Support of arbitrarily long terrains is needed in order to allow the vehicle to accelerate until it reaches its maximum steady state speed on the terrain or in order to simulate an actual vehicle traverse (including turns and up/down/side slopes) over an arbitrary topography terrain. Complex terrain topography includes:

1. Variable terrain vertical height as a function of the X and Y horizontal terrain coordinates. The resolution should be smaller than the smallest dimension of the vehicle running gear (such as tire or track segment).
2. Sloped terrains: positive and negative long slopes and side slopes.
3. Roughness specified by the spectrum of wave height (amplitude) versus wave length in two directions. The smallest wave length must be about  $1/10^{\text{th}}$  of the smallest dimension of the running gear.
4. Ditches specified by depth, width, and spacing distribution.
5. Bumps specified by depth, width, and spacing distribution.

A capability of modeling soft-soil complex topography terrains of arbitrary length is implemented in the DIS software tool based on a moving soil patch technique [2]. Using this technique particles which are far behind the vehicle are continuously eliminated and then reemitted as new particles in front of the vehicle. The terrain is defined using an  $i$ - $j$  ordered quadrilateral grid along with an emitter surface, a leveling surface, and a sink surface (Figure 26). The simulation starts by filling a rectangular range, say from  $i_1$  to  $i_2$  and  $j_1$  to  $j_2$ , where the  $i$  index is along the length of the soil patch and  $j$  is along the width, on the  $i$ - $j$  terrain surface with DEM particles up to a desired depth. Side wall surface at  $j = j_1$  and  $j = j_2$  along with the sink and emitter surfaces keep the particles inside the soil box. Then, the initial particles are compressed and leveled from the top using the terrain surface such that the same terrain topography is impressed on the soft-soil. Next, the sink, emitter, and leveling surfaces are enabled and moved along with the center of the vehicle. When a particle touches the sink surface behind the vehicle it is immediately disabled and then reemitted as a new particle from a random point on the emitter surface in front of the vehicle. The leveling surface levels and compacts the DEM particles that are emitted from the emitter surface. This effectively moves the soil patch along with the vehicle on the terrain. Since the sink, emitter and leveling surfaces all follow the underlying terrain's  $i$ - $j$  surface, the topography of the soft soil patch follows the topography of the terrain's  $i$ - $j$  surface. Figure 27 and Figure 23 show snapshots of typical vehicle simulations on complex topography terrains with terrain roughness, turns, and variable slope. Also, note that the complex topography moving soil patch technique has the capability of embedding rocks in the soil (Figure 23). The rocks are treated as another type of DEM particles and thus can interact with the moving soil patch surfaces and the vehicle components in a similar way as the DEM soil particles.

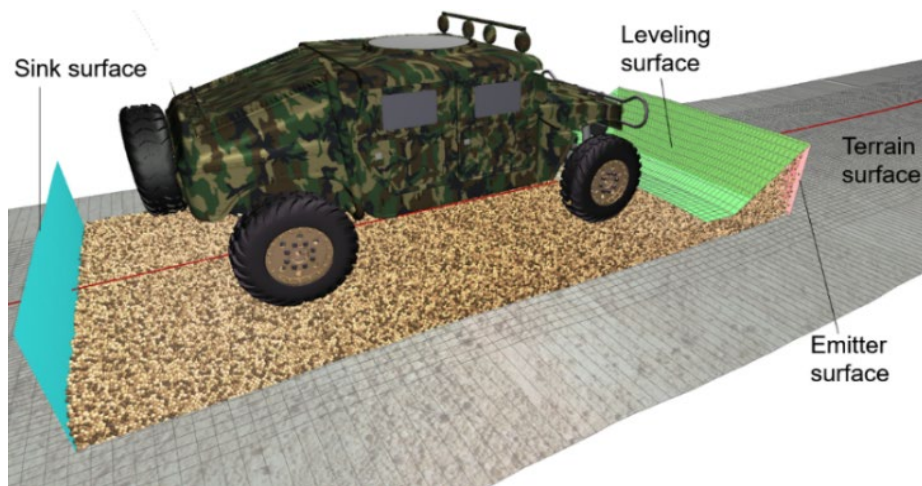


**Figure 26** DIS moving DEM complex topography soil patch modeled using an  $i$ - $j$  ordered quadrilateral grid representing the terrain's surface, an emitter surface, a leveling surface, and a sink surface. The complex topography moving soil patch can be used with soil particles and/or gravel/rock particles.



**Figure 27** Coupled DIS MBD/DEM simulation of a wheeled vehicle using a complex topography moving soil patch and about 1M particles which includes up/down slopes, turns, and surface roughness.

### 1.10 Ability to represent all types and sizes of worldwide vegetation

Vegetation models used in ground vehicle mobility must include the following effects:

1. Effect of vegetation root (below ground vegetation) stretching, slipping, and breaking on soil strength. In general soil strength increases with root size, depth, and root-area ratio (fraction of the soil cross sectional area that is occupied by roots per unit area of the vertical orthogonal projection of the above ground biomass [27]).
2. Frictional contact between the vegetation and vehicle and the vegetation and the soil. This includes on ground vegetation such as fallen leaves and grass and above ground vegetation stems.
3. Axial, bending, and torsional stiffness and damping of above ground vegetation.
4. Breaking strength of the above ground vegetation under axial, bending or torsional loads.
5. Maximum axial force and/or bending moment required to pull the vegetation from the soil.
6. Ability to predict vehicle mobility over fallen trees and branches.

Vegetation can be highly compliant such as grass, bushes, and crops, semi-compliant such as small-trees, and stiff such as medium and large tree. In general, vegetation mechanical properties depend on the vegetation type, stem diameter, temperature and moisture content. It was agreed in the AVT-28 committee to use the USNVC (US National Vegetation Classification) [28] vegetation classification system to identify the vegetation from a mechanical point of view. USNVC was chosen due to its widespread use,

and the fact that it covers most types of world-wide vegetation including natural and cultural vegetation (including grass, shrubs, crops, small trees, and large trees). USNVC [28] classifies plant species based on their structure, form, and species composition (assemblage of plant species that co-occur in an area). Those characteristics roughly correspond to similar mechanical properties within each vegetation sub-class. The USNVC vegetation classes are:

1. Tropical forest & woodland (10 sub-classes).
2. Shrub & herb vegetation (12 sub-classes).
3. Desert & semi-desert (3 sub-classes).
4. Polar & high montane scrub, grassland & barrens (3 sub-classes).
5. Aquatic vegetation (6 sub-classes).
6. Open rock vegetation (3 sub-classes).
7. Agricultural & developed cultural vegetation (13 sub-classes).

Therefore, there are about 50 vegetation sub-classes/types in the USNVC. In addition, each sub-class can have a number of divisions which may be important from a mechanical point of view. The vehicle and vegetation response quantities of interest include:

1. 3D deflection and breakage of the vegetation stem. Note that a stem can break either at the base when the stem and its roots are pulled from the soil or it can break at a point along the stem length.
2. 3D interaction forces on the vehicle due to the vegetation at any vehicle speed.
3. GO/NOGO (can the vehicle override the vegetation given the available engine power and the maximum traction the soil can support).
4. Vehicle - vegetation override force at any vehicle speed and impact direction. The override force must be smaller than the force which will cause permanent deformation to the vehicle body.
5. Vehicle - vegetation resistance force at any vehicle speed and impact direction.
6. Rut depth and width after the vegetation stem is pulled from ground.

Figure 28 shows a DIS simulation of a wheeled vehicle over a complex topography crop/grass covered terrain. The vegetation blades are modeled using beam finite elements which are laid out over a complex topography road surface (see Section 1.9). The beam elements include the effects of axial, bending, and torsional stiffness/damping, aerodynamic resistance; and bending and axial breaking strengths. Note that the bending and axial strengths at the beam base are due to the contact of the vegetation root and stem with the soil and therefore are typically different than the bending and axial strengths along the beam. Figure 29 shows a DIS simulation combining the DEM model for the soil with the beam element vegetation model. The DEM maximum inter-particle adhesive strength versus plastic strain curve is modified in order to account for the increase of soil strength due to roots.



**Figure 28** DIS simulation of a wheeled vehicle over a crop/grass covered terrain. The right figure shows the breaking of the breaking of the vegetation blades behind the vehicle.

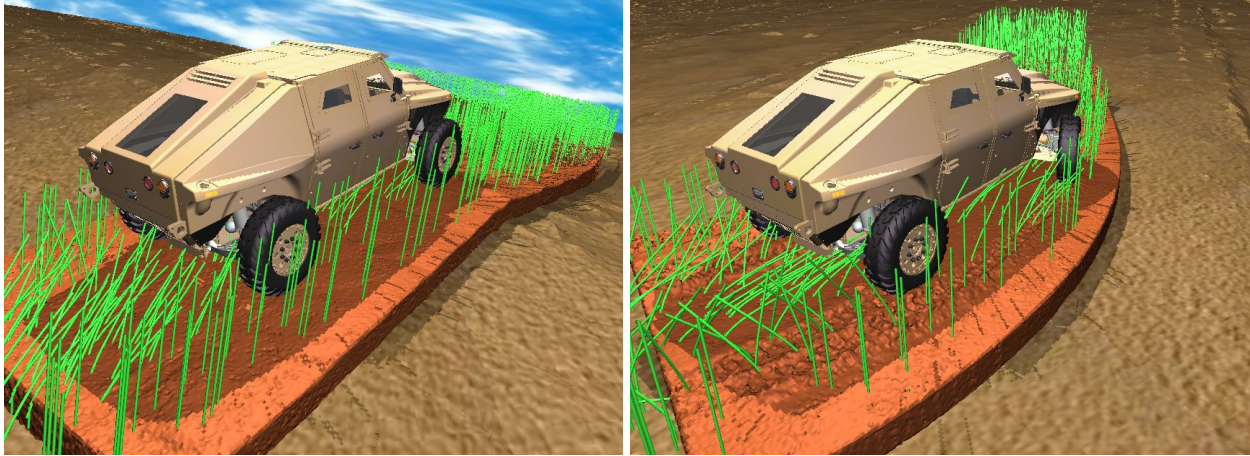


**Figure 29** DIS simulation combining the vegetation model with the soft soil DEM model.

### *1.11 Ability to represent natural and urban obstacles*

Natural obstacles (excluding vegetation) include large rocks and fallen trees (similar in size or larger than the radius of the vehicle tires or track wheels). Urban obstacles include poles (Figure 30), walls (including brick, concrete, and sheet metal), fences (including metal wire, metal bars, and wood), bridges, tunnels, other vehicles, debris, and small structures. Obstacle models must include the following effects:

1. Obstacle geometry.
2. Mechanical compliance and strength of the obstacle.
3. Interaction of the obstacle with the soil. The obstacle can be embedded/buried in the soil.
4. Mechanical properties at the interface between the soil and the obstacle, including adhesion and friction.
5. Friction between the obstacle and the vehicle surfaces (tires, tracks, and/or vehicle body).



**Figure 30** DIS simulation of tracked vehicle overriding a pole embedded in the DEM soil.

The response quantities of interest include:

1. 3D motion, deflection, and breakage strength (under bending and/or axial loads) of the obstacle.
2. 3D interaction forces between the obstacle and the vehicle.
3. GO/NOGO (can the vehicle override the obstacle given the available engine power and the maximum traction the soil can support).

4. Override force at any vehicle speed and impact direction. The override force must be smaller than the force which will cause permanent deformation to the vehicle body.
5. Resistance force at any vehicle speed and impact direction.
6. Soil rut depth and width created by the obstacle.

### *1.12 Ability to read the terrain input data from GIS software tools*

The terrain map is rasterized into cells of nearly the size of the vehicle (e.g. 10 m x 10 m). For each terrain cell, the following input parameters from Geographic Information Systems (GIS) software tools can be specified and read by the CT software tools in order to calculate the vehicle mobility measures over that grid cell:

- Terrain topography.
  - Elevation above a known reference (such as sea level).
  - Slope/grade and slope/grade direction.
  - Roughness which can be measured by spectrum of wave length versus roughness/height amplitude in two directions.
  - Maximum trench (negative obstacle) width, depth, and spacing.
  - Maximum bump (positive obstacle) width, depth, and spacing.
- Soil: 1 to 3 layers each having:
  - USCS soil type, moisture, and temperature (those will map to the soil complex terramechanics model material parameters such as cohesion, friction, density, damping, and viscosity).
  - Layer thickness.
- Heterogeneous terrain.
  - Type: Embedded rocks, embedded debris, soil patches.
  - Shape distribution.
  - Size distribution.
  - Spacing distribution.
- Land use: agricultural; urban terrain; grass land; bare ground; forest swamp; water, etc.
- Vegetation.
  - USNCS vegetation type.
  - Roots sizes and spacing distributions.
  - Stems sizes and spacing distributions.
- Urban obstacles, including: roads (paved asphalt, paved concrete, dirt, gravel, ...); ditches; buildings; poles; walls (brick, concrete, etc.); fences; structures; bridges; tunnels; vehicles; debris.

### *1.13 Ability to generate terrain mobility maps and display the maps in GIS software tools*

One of the main functions of the NG-NRMM software tool is to help mission planners, drivers, or vehicle AI systems select the optimum vehicle route on a terrain map based on the mission requirements and real-time terrain conditions. In order to perform this function the NG-NRMM software tool must be able to generate a map of the terrain colored by the various mobility measures such as speed-made-good and fuel-consumption. The input to the NG-NRMM software tool is the GIS terrain map which consists of terrain cells/units with each cell having the properties identified in Section 1.12. Typical terrain maps can be 20x20 km and typical grid cell dimensions are 10x10 m. Therefore, a typical terrain map can have millions of grid cells. Each cell can potentially have a unique combination of GIS terrain variables such as slope, soil type, moisture content, vegetation type, roughness, obstacles, etc. Therefore, if one CT vehicle mobility simulation is performed for each terrain cell, millions of simulations maybe needed to generate

the terrain mobility map. Since each CT simulation can have millions of DOFs to model the soil and vehicle, and at current computer speeds may require on the order of at least a day to run, this can translate into millions of days of computer time. In order to reduce the required number of simulations and computer time, an expert system along with a DOE strategy and response surface technique can be used.

Instead of running a CT simulation for each terrain cell, runs are performed for selected combinations of terrain variables within the range of each variable. The results of the runs can then be aggregated using the rules of the expert system along a multivariable response surface (surrogate model) [29] which can interpolate the DOE points to generate the vehicle response for the desired combination of GIS terrain variables. Figure 31 shows a GIS terrain map colored using speed-made-good generated by the CT NG-NRMM prototype software tool.

In addition, the value of each GIS terrain variable for each terrain cell is uncertain and can be represented using a probability distribution (such as a normal distribution). Therefore, the output mobility measures are also uncertain and can also be represented by a probability distribution. In order to generate the output mobility measures probability distributions for each terrain cell, a Monte Carlo process where the surrogate model is run for each terrain cell using 1000's of combinations of the various terrain variables within the range of each variable probability distribution on the terrain cell, then the output mobility measures for all the runs are used to approximate the probability distribution of the mobility measures on the terrain cell [29]. The terrain can then be colored using the mobility measure at a desired probability level (Figure 32). For example, the 90% probability speed-made-good map means that there a 90% probability that the maximum speed will be greater than or equal to the speed in the map.

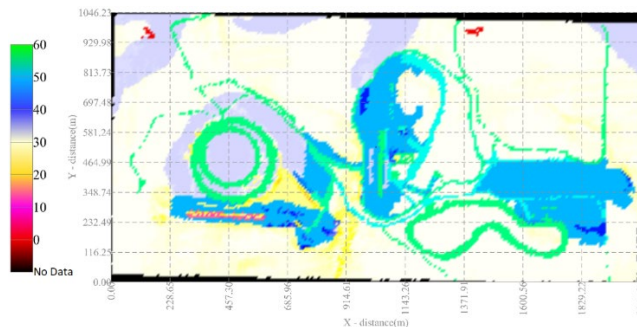


**Figure 31** DIS generated deterministic speed-made-good GIS terrain map in km/hr considering the soil type, positive terrain slope, and terrain RMS roughness for a typical wheeled vehicle.

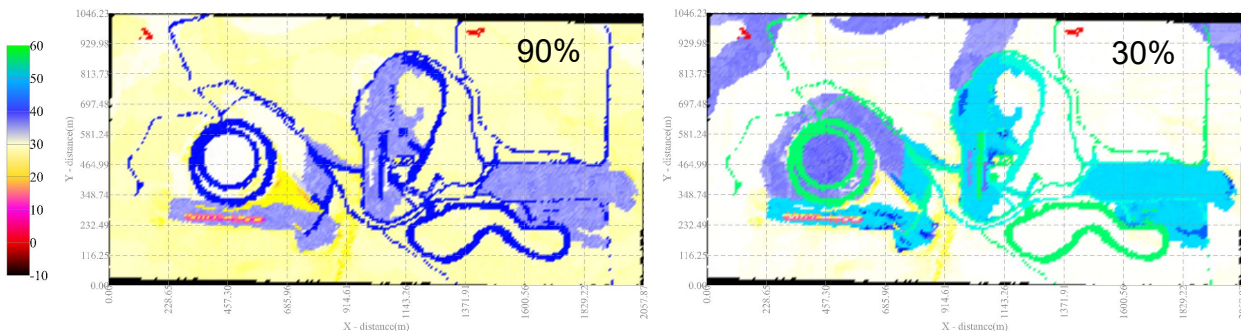


**Figure 32** DIS generated non-deterministic speed-made-good GIS terrain maps at 90% and 30% probability distribution levels in km/hr considering the soil type, positive terrain slope, and terrain RMS roughness for a typical wheeled vehicle. 90% probability speed-made-good map means that there a 90% probability that the maximum speed will be greater than or equal to the speed in the map.

### *1.14 Ability to conduct coupled simulations with multibody dynamics software for modeling the vehicle*

The CT terramechanics software tool must be integrated with MBD vehicle models such that the integrated software tool has the following vehicle modeling capabilities:

1. Ability to model tires. The tire model must be able to account for the effect of inflation pressure (for pneumatic tires), tire construction, and tread pattern/depth on vehicle mobility. Under-inflated tires typically yield high vehicle mobility on soft soil and low mobility on hard terrains, while the reverse is true for tire inflated to the nominal pressure. The tire model must accurately represent the tire construction including layout and material properties of the ply, belt, and bead reinforcements and the rubber matrix. In the finite element (FE) tire model integrated into the CT prototype [11], the tire rubber matrix is modeled using 8-node brick elements with a hyper-elastic material model. The tire reinforcements belt, ply, and bead along the circumference direction, and the ply along meridian direction are modeled using thin beam elements which are embedded (share the same nodes) as the rubber brick elements (Figure 33). A polygonal surface representing the tread is attached to the outer surface of the rubber brick elements as a proxy contact surface (Figure 33). Figure 34 shows a snapshot of a multibody vehicle model with FE tires colored using the lateral shear stress. Figure 35 shows snapshots from a simulation of a multibody dynamics vehicle model with an FE tire with a proxy contact surface representing the tread modeled going over a DEM soft soil terrain. The contact forces on a tread point are transferred to the FE nodes of the closest element by distributing the force based on the distance between the point and each of the element nodes. The tire model must be able to accurately predict for both hard and soft soil terrains the following tire response quantities as well as resulting rut depth (for soft soils) for any internal tire pressure:
  - a. Normal load versus deflection and contact footprint length. Also, the rut depth on soft soil
  - b. Rolling resistance at any normal load and speed.
  - c. Longitudinal force versus slip at any normal load and speed.
  - d. Lateral force and self-aligning torque at any slip angle, normal load and speed.
2. Ability to model segmented tracks including single pin and double pin tracks (Figure 36). This includes the effects of track shoe grouser pattern and pad material on vehicle mobility. It also includes the effect of track bushings stiffness and track pin friction torque.
3. Ability to model continuous belt-type tracks (Figure 36). This includes effect of track construction (including layout and material properties of the longitudinal and lateral track reinforcements and the rubber matrix), and track tread pattern.
4. Ability to model the interaction of any vehicle part with the terrain. Those include: underbody; legs; blades and buckets; tines for tilling the soil and for mine sweeping (e.g. Figure 37).
5. Ability to model the vehicle systems necessary for mobility, including: suspension system; steering system; driveline (shafts, splined shafts, U-joints, CV-joints, revolute joints, gear box, torque converter, clutch, transfer cases, differentials, and axles); engine; brakes; and vehicle controls such as: ESC (Electronic Stability Control), ABS (Antilock Braking System), and VI (Vehicle Intelligence).
6. Ability to model vehicle payloads, including: cargo containers; equipment; other vehicles; human occupants; liquid filled tanks; and trailers (e.g. Figure 38).
7. Ability to model the various types of vehicle maneuvers on any terrain in the full vehicle speed range. Those include:
  - a. Steering, including:

- i. Closed-loop steering tests including: single and double lane change, obstacle avoidance, and turns (e.g. 90° turn).
- ii. Open-loop steering tests including: J-turn and fishhook turn.
- b. Constant radius turning/cornering.
- c. Neutral axis spin for tracked and legged vehicles.
- d. Braking. This includes predicting the stopping distance from any initial speed.
- e. Crossing obstacles such as half-rounds.
- f. Traveling on a rough terrain with known roughness spectrum (roughness height versus wave length).
- g. Traveling in a prescribed path and speed on any given terrain (including side slopes, long slopes, and complex topography terrains).

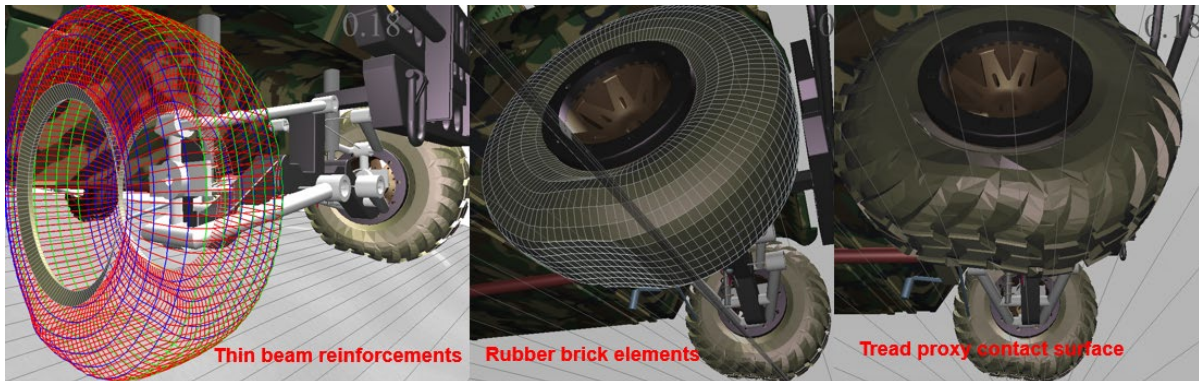


**Figure 33** Finite element tire reinforcements (left), rubber brick elements (center), and tread proxy contact surface (right).

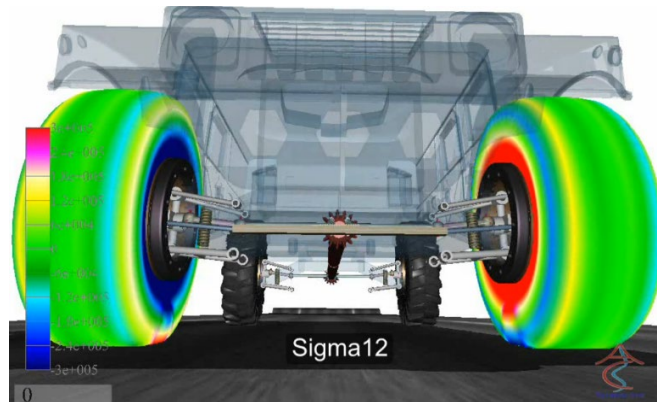


**Figure 34** Snapshot from a DIS simulation of the multibody vehicle with finite element flexible tires colored using the lateral shear stress.

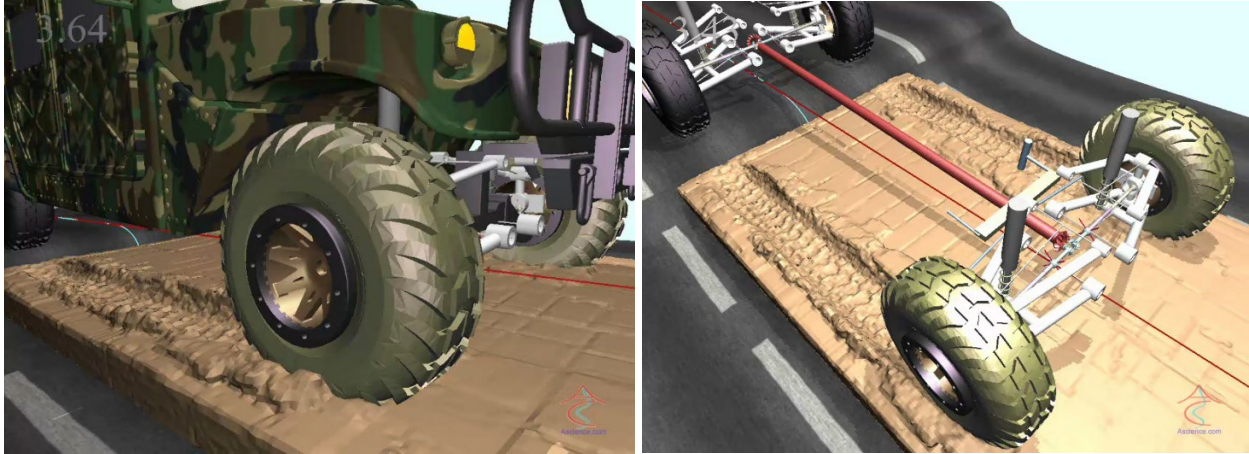


**Figure 35** Snapshots of a DIS vehicle simulation with a flexible tire having a complex tread pattern running on DEM soft soil.

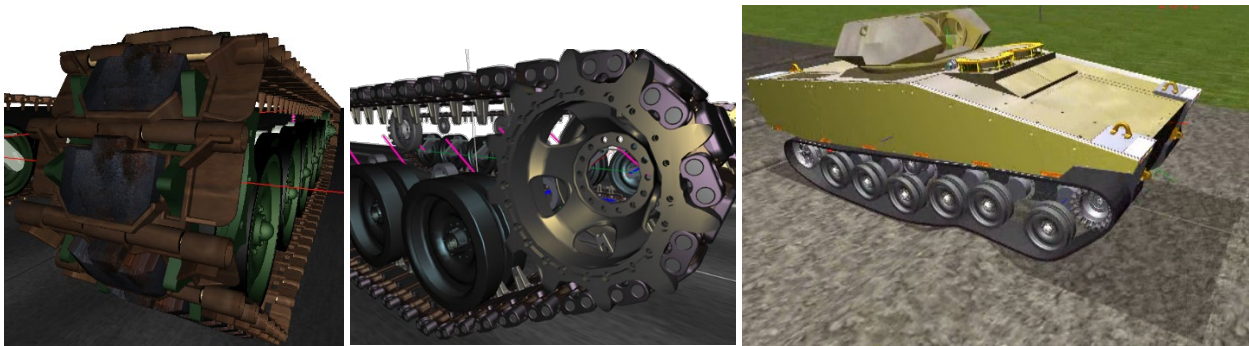


**Figure 36** Typical single pin segmented track (left), double pin track segmented track (center); and DIS simulation of a belt-type tracked vehicle (right).

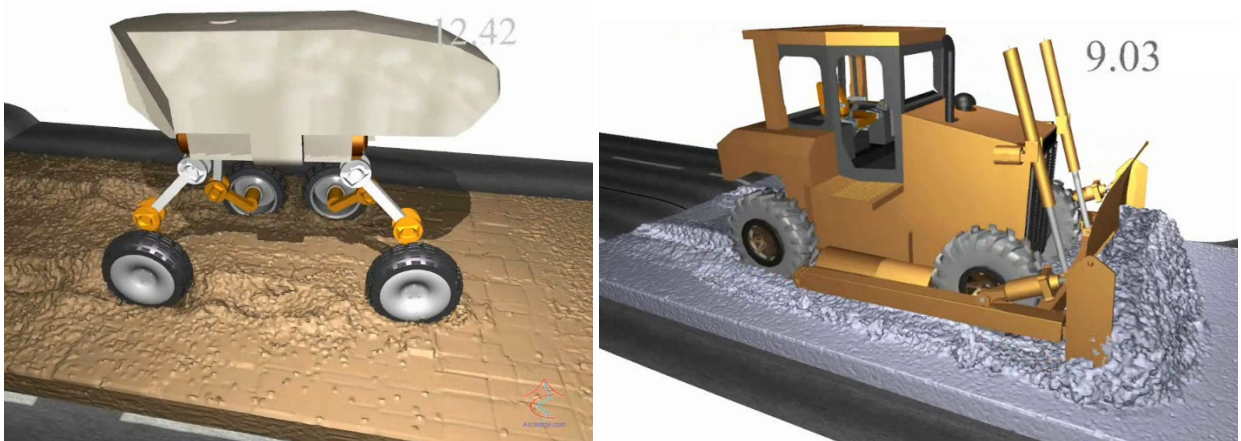


**Figure 37** DIS simulation of a 4-legged walking vehicle on soft DEM soil (left) and a bulldozer digging through a cohesive soft soil representing snow (right).

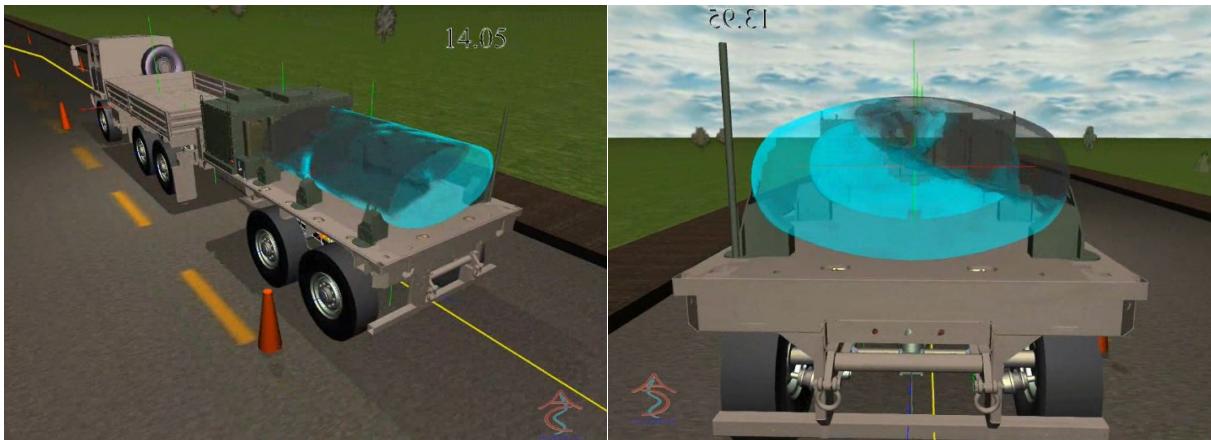


**Figure 38** Snapshots of a DIS simulation of a military tanker truck-trailer vehicle carrying a water tank with the water modeled using SPH.

## 2. Concluding Remarks

The 14 complex terramechanics (CT) software tools requirements recommended in the NATO RTG-248 were presented in this paper along with example simulations from a CT prototype software tool which attempts to satisfy the requirements in order to demonstrate that the requirements are achievable in a relatively short term. The NG-NRMM software tool requirements developed in RTG-248 were compiled into an initial NATO STANREC. A new NATO RTG-327 was formed in 2019 to upgrade and manage this NATO STANREC with the goal of developing it into a NATO STANAG (Standardization Agreement). A 3-day Cooperative Demonstration of Technology (CDT-308) was held in September 2018 at the Keweenaw Research Center in Houghton, Michigan, USA to demonstrate the NG-NRMM technology development and to conduct a V&V exercise comparing software tools vehicle response predictions on both hard and soft soil terrains to actual vehicle tests [30, 31]. Future developments NG-NRMM will focus on the following tasks:

1. Calibrating and validating the terramechanics models for all USCS soil types, with 0 to 100% moisture content, and  $-40^{\circ}\text{C}$  to  $40^{\circ}\text{C}$  temperatures. The calibration will be carried out using small-scale terramechanics experiments. The validation will be carried out using full-scale military vehicles of various sizes and types including wheeled and tracked vehicles.
2. Calibrating and validating the vegetation models for all USNVC vegetation types, temperature range, and moisture content range.
3. Develop the stochastic mobility expert system to enable predicting the vehicle mobility measures on any GIS terrain which may include all the GIS terrain variables listed in Section 1.12.
4. Improving the modeling fidelity and computational efficiency of the various NG-NRMM underlying computational models including: soil, multiple soil layers, heterogeneous terrains, water covered terrains, vegetation, and urban obstacles.

## Acknowledgements

The authors would like to thank the AVT-RTG-248 Complex Terramechanics team members: Russ Alger, Ole Balling, Andreas Becker, Scott Bradley, Craig Foster, Susan Frankenstein, Michael McCullough, Dan Negrut, Phumlane Nkosi, Jon Preston-Thomas, David Reinecke, Radu Serban, Sally Shoop, Tom von Sturm zu Vehlingen, and Xiaobo Yang, for their valuable feedback and numerous discussions. The first author would like to acknowledge the financial support from the U.S. Army TARDEC through Contracts W911NF11D00010311/TCN15011, FA807514D0014/SFP1247915, and W56HZV18C0115.

## References

1. *DIS (Dynamic Interactions Simulator)*. 2019 [cited 2019; Available from: <http://www.ascience.com/ScProducts.htm>].
2. Wasfy, T.M., P. Jayakumar, D. Mechergui, and S. Sanikommu, *Prediction of Vehicle Mobility on Large-Scale Soft-Soil Terrain Maps Using Physics-Based Simulation*, in *GVSETS 2016, 2016 NDIA Ground Vehicle Systems Engineering and Technology Symposium, Modeling & Simulation, Testing and Validation (MSTV) Technical Session*. 2016: Novi, MI.
3. Wasfy, T.M., Wasfy, H.M. and Peters, J.M., *High-Fidelity Multibody Dynamics Vehicle Model Coupled with a Cohesive Soil Discrete Element Model for predicting Vehicle Mobility*, in *11th International Conference on Multibody Systems, Nonlinear Dynamics, and Control*. 2015, ASME: Boston, MA.
4. Wasfy, T.M., Ahmadi, S., Wasfy, H.M., and Peters, J.M., *Multibody Dynamics Modeling of Sand Flow from a Hopper and Sand Angle of Repose*, in *9th International Conference on Multibody Systems, Nonlinear Dynamics, and Control*. 2013, ASME: Portland, OR.
5. Ahmadi, S., T.M. Wasfy, H.M. Wasfy, and J.M. Peters, *High-Fidelity Modeling of a Backhoe Digging Operation using an Explicit Multibody Dynamics Code with Integrated Discrete Particle Modeling Capability*, in *2013 International Design Engineering Technical Conference, 9th International Conference on Multibody Systems, Nonlinear Dynamics, and Control (MSNDC)*. 2013, ASME.
6. Wasfy, T.M. and J. O’Kins, *Finite Element Modeling of the Dynamic Response of Tracked Vehicles*, in *International Design Engineering Technical Conferences, 7th International Conference on Multibody Systems, Nonlinear Dynamics, and Control*. 2009, ASME: San Diego, CA.
7. Wasfy, T.M., J. O’Kins, and S. Smith, *Experimental Validation of a Time-Accurate Finite Element Model for Coupled Multibody Dynamics and Liquid Sloshing*. SAE 2007 Transactions, Journal of Passenger Cars: Mechanical Systems, 2008(Document Number: 2007-01-0139).
8. Wasfy, T.M., O’Kins, J. and Smith, S., *Experimental Validation of a Coupled Fluid-Multibody Dynamics Model for Tanker Trucks*. SAE International Journal of Commercial Vehicles, 2008. **1**(1): p. 71-88.
9. Wasfy, T.M. and H.M. Wasfy, *Object-oriented environment for dynamic finite element modeling of tires and suspension systems*, in *2006 Mechanical Engineering Congress and Exposition Conference*. 2006, ASME: Chicago, IL.
10. Wasfy, T.M., *Modeling spatial rigid multibody systems using an explicit-time integration finite element solver and a penalty formulation*, in *Proceeding of the DETC: 28th Biennial Mechanisms and Robotics Conference*. 2004, ASME International: Salt Lake, Utah.
11. Wasfy, T.M.a.L., M.J., *Modeling the dynamic frictional contact of tires using an explicit finite element code*, in *5th International Conference on Multibody Systems, Nonlinear Dynamics, and Control*. 2005, ASME: Long Beach, CA.
12. *ASTM Standard D6128-16, Standard test method for shear testing of bulk solids using the Jenike shear cell*. 2016, ASTM International: West Conshohocken, PA, USA.
13. *ASTM D4767-11, Standard Test Method for Consolidated Undrained Triaxial Compression Test for Cohesive Soils*. 2011, ASTM International: West Conshohocken, PA.
14. *ASTM D2850-15, Standard Test Method for Unconsolidated-Undrained Triaxial Compression Test on Cohesive Soils*. 2015, ASTM International: West Conshohocken, PA.
15. Apfelbeck, M., S. Kuß, B. Rebele, and B. Schäfer, *A systematic approach to reliably characterize soils based on Bevameter testing*. Journal of Terramechanics, 2011. **48**(5): p. 360-371.

16. Bilanski, W.K. and A.L.L. Esperance, *An investigation of the bevameter soil physical measurements in the prediction of soil tool draft*. Journal of Terramechanics, 1990. **27**(1): p. 41-50.
17. Wong, J.Y., *Terramechanics and Off-Road Vehicle Engineering (Second Edition)*. 2010, Oxford, UK: Elsevier.
18. Shoop, S., *Terrain Characterization for Trafficability*. 1993, US Army Corps of Engineers: Cold Regions Research & Engineering Laboratory (CRREL).
19. Roy, A., *Experimental Validation of Non-Cohesive Soil using Discrete Element Method*, in *Department of Mechanical Engineering*. 2018, Indiana University Purdue University Indianapolis: Indianapolis, IN. p. 67.
20. Senatore, C., M. Wulfmeier, J. MacLennan, P. Jayakumar, and K. Iagnemma, *Investigation of stress and failure in granular soils for lightweight robotic vehicle application*, in *NDIA Ground Vehicle Systems Engineering and Technology Symposium*. 2012, NDIA: Novi, MI.
21. ASAE, *Soil cone penetrometer*, in *Standard ASAE S3 13.2*. 1985, American Society of Agricultural Engineers.
22. SAE, *Off-road vehicle mobility evaluation*, in *SAE Recommended Practice Handbook Supplement*. 1967, Society of Automotive Engineers (SAE): Warrendale, PA.
23. Wasfy, T.M., P. Jayakumar, D. Mechergui, and S. Sanikommu, *Prediction of Vehicle Mobility on Large-Scale Soft-Soil Terrain Maps using Physics-Based Simulation*. International Journal of Vehicle Performance, 2018. **4**(4).
24. ASTM, *ASTM Standard D2487, Standard Practice for Classification of Soils for Engineering Purposes (Unified Soil Classification System)*. 2000, ASTM International: West Conshohocken, PA.
25. ASTM, *ASTM D4318-10, Standard Test Methods for Liquid Limit, Plastic Limit, and Plasticity Index of Soils*. 2010, ASTM International: West Conshohocken, PA.
26. Wasfy, T.M., Wasfy, H.M. and Peters, J.M., *Coupled Multibody Dynamics and Smoothed Particle Hydrodynamics for Modeling Vehicle Water Fording*, in *11th International Conference on Multibody Systems, Nonlinear Dynamics, and Control*. 2015, ASME: Boston, MA.
27. Baets, S.D., J. Poesen, B. Reubens, K. Wemans, J.D. Baerdemaeker, and B. Muys, *Root tensile Strength and Root Distribution of Typical Mediterranean Plant Species and their Contribution to Soil Shear Strength*. Plant and soil, 2008. **305**: p. 207-226.
28. *US National Vegetation Classification (USNVC)*. 2019 [6/22/2019].
29. Choi, K.K., P. Jayakumar, M. Funk, N. Gaul, and T.M. Wasfy, *Framework of Reliability-Based Stochastic Mobility Map for Next Generation NATO Reference Mobility Model*. ASME Journal of Computational and Nonlinear Dynamics, 2019. **14**(2).
30. Letherwood, M., P. Jayakumar, D. Gorsich, P. Rogers, M. Hoenlinger, W. Mayda, M. McCullough, S. Bradley, R. Alger, R. Serban, O. Balling, F. Homaa, T. Wasfy, N. Gaul, M. Bradbury, E. Pesheck, D. Reinecke, M. Hirschhorn, J. Wong, L. Bendtsen, M. Funk, R. Williams, and C. Mueller, *Cooperative Demonstration of Technology (CDT- 308): Next-Generation NATO Reference Mobility Model (NG-NRMM)* ed. M. Letherwood, et al. 2019: NATO Research and Technology Organization.
31. *NG-NRMM CDT*. 2019 [cited 2019 August 2019]; Available from: <https://www.mtu.edu/cdt/>.